# A Minimal Solution to the Generalised 3-Point Pose Problem

David Nistér
Sarnoff Corporation
CN5300, Princeton, NJ 08530, USA
dnister@sarnoff.com

## Abstract

*It is a well known classical result that given the image projections of three known world points it is possible to solve for the pose of a calibrated perspective camera to up to four pairs of solutions. We solve the generalised problem where the camera is allowed to sample rays in some arbitrary but known fashion and is not assumed to perform a central perspective projection. That is, given three back-projected rays that emanate from a camera or multi-camera rig in an arbitrary but known fashion, we seek the possible poses of the camera such that the three rays meet three known world points. We show that the generalised problem has up to eight solutions that can be found as the intersections between a circle and a ruled quartic surface. A minimal and efficient constructive numerical algorithm is given to find the solutions. The algorithm derives an octic polynomial whose roots correspond to the solutions. In the classical case, when the three rays are concurrent, the ruled quartic surface and the circle possess a reflection symmetry such that their intersections come in symmetric pairs. This manifests itself in that the odd order terms of the octic polynomial vanish. As a result, the up to four pairs of solutions can be found in closed form. The proposed algorithm can be used to solve for the pose of any type of calibrated camera or camera rig. The intended use for the algorithm is in a hypothesise-and-test architecture.*

## 1. Introduction

Solving for the pose of a camera given the images of known points in the world is a fundamental task in computer vision in general and structure from motion in particular. Solutions exist for most traditional camera models, such as for example orthographic, weak perspective [2], affine, projective [5, 11] and calibrated perspective [8, 10].

In the case of a calibrated perspective camera, the images of three known world points constrain the possible poses of the camera to up to four pairs of solutions. At most one solution from each pair is valid according to the orientation constraints and the other solution is the reflection of the camera centre across the plane of the three points.

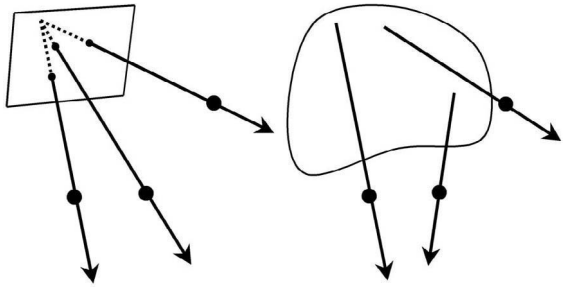

Figure 1: Left: The well known classical problem is to solve for the pose of three concurrent rays, such that the rays meet three known world points. Right: We solve the generalised problem of finding the rigid pose of three arbitrary rays emanating from a generalised camera geometry, such that the three rays meet three known world points. This lets us deal with any of the recently very popular camera geometries that do not adhere to a central perspective model, such as for example a camera facing an arbitrarily shaped mirror.

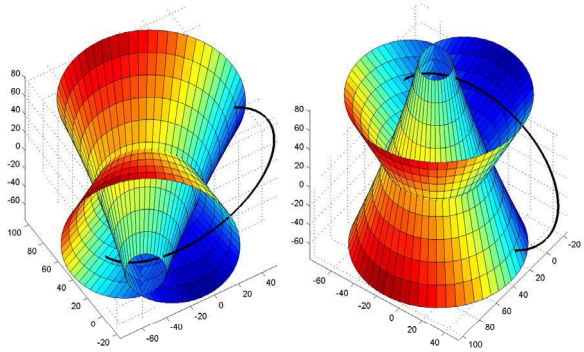

Figure 2: It is possible to think of the problem as that of finding the intersections between a ruled quartic surface and a circle. There can be up to eight such intersections. The figure shows four intersections at the top and four at the bottom of the surface.

Prepared through collaborative participation in the Robotics Consortium sponsored by the U. S. Army Research Laboratory under the Collaborative Technology Alliance Program, Cooperative Agreement DAAD19-01-2-0012. The U. S. Government is authorized to reproduce and distribute reprints for Government purposes notwithstanding any copyright notation thereon.



IEEE COMPUTER SOCIETY

To find the solutions is the well known classical 3-point perspective pose problem. It was considered already by Lagrange and the first closed form algebraic solution appears to be by Grunert [9]. Grunert's solution and those of several other authors are compared in [10]. For more on the history of the pose problem, see [8].

Many more point correspondences than the minimal three are needed to obtain robust, accurate and automatic solutions. The strength of the minimal solutions in structure from motion is due to their application in hypothesise-and-test architectures such as [6, 13]. Many minimal solutions are carried out and the multiple hypotheses thus generated are scored based on their support over the complete set of observations.

We will solve a generalisation of the classical 3-point perspective pose problem. The generalisation is motivated by the recent popularity of generalised camera geometries that do not adhere to the central perspective model and do not correspond to a single viewpoint. We consider a generalised camera that samples the light field or plenoptic function [1] in some arbitrary but known fashion. An illustration is given in Figure 1. In practice, the generalised camera can for example be a camera together with a curved mirror such as a catadioptric or dioptric system, a multi-camera rig [3, 14] or a compound camera made of many individual sensing elements rigidly attached to each other.

A framework for generalised cameras is given in [7] along with a calibration method. Calibration in this case means that given an image point we know the ray of points in the coordinate system of the camera that projects to the image point. If the generalised camera has imaged three known world points, the calibration immediately gives us the three rays that project to the image points. The generalised 3-point pose problem is then to find the rigid transformation of the three rays, such that they all meet their corresponding world points.

It is noteworthy that in solving this problem, we can treat all generalised cameras in a unified way, without assuming a specific type of camera model. Without calibration, this would be very hard to accomplish, since in the uncalibrated case, one would typically have to settle on a specific camera model in which to solve for the parameters. By supposing that the calibration is known, we can essentially relegate all specifics about the camera model to the calibration procedure, which can be carried out in a controlled environment.

We will show that the generalised 3-point pose problem can have up to eight solutions that correspond to intersections between a circle and a ruled quartic surface as illustrated in Figure 2. The intersections of the ruled quartic surface with the plane of the circle is a quartic curve. A plane quartic curve in general has eight intersections with a circle if complex solutions are taken into account. In the classical case, when all three rays are concurrent, the problem attains a symmetry that groups the eight solutions into the well known four pairs of symmetric solutions.

The rest of the paper is organised as follows. Section 2 highlights a relevant classical theorem. In section 3 we present the main idea of our solution approach. The concepts of the solution are outlined in Sections 4 and 5. The algorithm steps are stated in Section 6 and then given in detail in Section 7. Section 8 draws the link to the classical case. Section 9 discusses the orientation constraints, 10 gives an experimental verification and 11 concludes.

## 2. A Relevant Theorem

We will find Proposition 21 of book III of Euclid's Elements [4] relevant to our discussion:

**Theorem 1** *In a circle, all inscribed angles subtending the same arc are equal.*

An illustration is given in Figure 3.

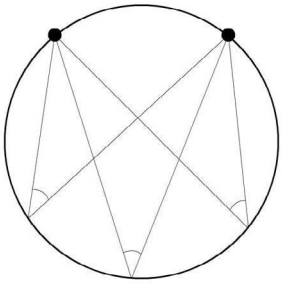

Figure 3: In a circle, all inscribed angles subtending the same arc are equal. We will find this highly relevant, since it corresponds to one of the two degrees of freedom that will remain when we study what happens when the constraints from only two of the rays are enforced.

## 3. Solution Approach

To solve our problem, we will first study how the constraints given by two of the three rays constrain the poses of the rigid bundle of rays with respect to the world. We will then see what this means in terms of the constraint from the third ray.

The pose has six degrees of freedom, three for rotation and three for translation. The constraint that a back-projected ray should pass through a known world point removes two degrees of freedom. Hence, two rays constrain the pose to two degrees of freedom. We will think of one of these degrees of freedom in terms of a transformation of the third world point and the other in terms of possible positions of the third back-projected ray. We will show that the first degree of freedom lets the third world point trace out a circle relative to the camera. We will then show that the other degree of freedom lets the third back-projected ray

trace out a ruled quartic surface in the world. The possible solutions for the pose correspond to the up to eight intersections between the circle and the ruled quartic surface.

# 4. The Circle

In this section, we describe the first of the two degrees of freedom that remain when we only enforce the constraints given by the first two rays. Consider one of the many possible poses of the rigid configuration of the three rays with respect to the three world points, such that the first two rays meet the first two world points. The two world points define a unique axis in space that passes through them both, see Figure 4. We now observe that we are free to rotate the configuration of world points around this axis while keeping the configuration of rays fixed, without violating the constraints given by the first two rays. This is the effect of one of our degrees of freedom. We are essentially only interested in how the rotation affects the third world point. As we rotate around the axis of the first two world points, the third world point describes a circle around the axis in a plane perpendicular to the axis. One can therefore think of the world coordinate system as containing the first two points and a circle. The situation is illustrated in Figure 4.

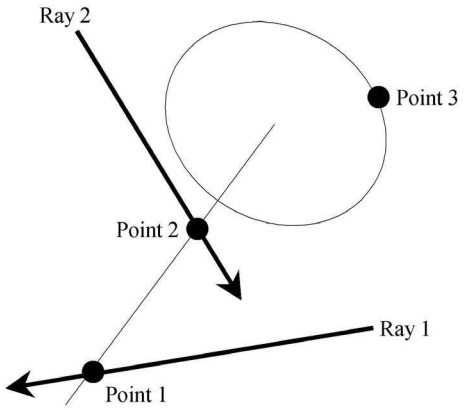


Figure 4: An illustration of the first of the two degrees of freedom that remain when we only enforce the constraints from the first two point correspondences. We are free to rotate the third world point around the axis defined by the first two world points, since this does not affect the constraints imposed by the first two rays. As we do this, the third world point describes a circle around the axis.

# 5. The Ruled Quartic Surface

In this section, we describe the second degree of freedom that remains when the constraints from the first two rays have been enforced. We assume that the back-projected rays are not all parallel. The case of parallel rays is essentially orthographic projection and the solutions are well known [2]. If the rays are not all parallel we can find two rays with distinct directions and choose them as the first two rays. They then have a unique common perpendicular direction. Moreover, there is a unique line in the perpendicular direction that meets both rays. We will refer to this line as the *perpendicular axis*. The situation is illustrated in Figure 5. If we consider an orthographic projection along the perpendicular axis, we get a situation corresponding to Theorem 1. More exactly, there is a rigid motion that revolves the perpendicular axis around on a cylinder while satisfying the contraints imposed by the first two rays. In addition to the perpendicular axis, the cylinder contains the first two world points. The revolving motion affects all planes perpendicular to the axis equally, hence the intuitive notion of an orthographic projection along the perpendicular axis.

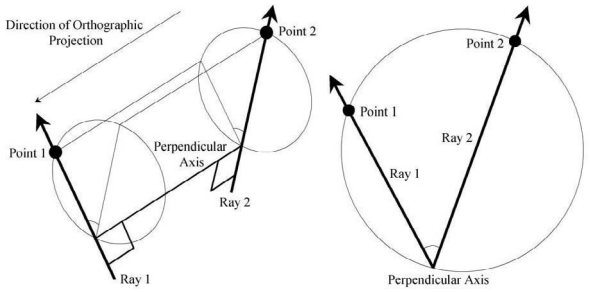


Figure 5: An illustration of the second degree of freedom. If we consider an orthographic projection (shown on the right) along the perpendicular axis of the first two rays, we see that the situation corresponds to Theorem 1. There is a set of Euclidean transformations that revolve the perpendicular axis around on a cylinder while satisfying the contraints imposed by the first two rays. We will find that this revolving motion causes the third ray to trace out a ruled quartic surface.

To determine how the revolving motion affects the third image ray, we now proceed to represent it algebraically. We will determine a family of transformations, where each transformation maps the world points to one of the valid positions traced out by the revolving motion. Note that this means that we will think of the problem 'in reverse', i.e. the transformations we will consider map the world points into the coordinate system of the image rays. We will find that the world points that can map onto the third ray lie on a ruled quartic surface, i.e. as we perform the revolving motion, the third ray traces out a ruled quartic surface.

## 5.1 Coordinate System

We first transform the rays and points to starting positions that will simplify the algebra. The starting positions are illustrated in Figure 6. Let the first ray coincide with the


IEEE COMPUTER SOCIETY

$y$-axis and let the perpendicular axis be the $z$-axis. Then, the origin is where the first ray meets the perpendicular axis and the axes are determined up to arbitrary signs. We then transform the points so that the first and second points take particular positions. Let the first point coincide with the origin. Then rotate around the origin such that the second world point lies on the line of intersection between the $xz$-plane and the $z$-plane of the second ray. There are typically two such locations for the second world point. For uniqueness, choose the point such that $x >= 0$. [1] This determines the coordinate system for the world points up to a rotation around the axis defined by the first two points. This rotation can be chosen arbitrarily and does not affect the coordinate representation of the circle.

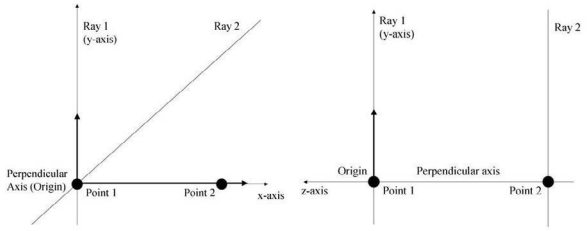


Figure 6: Two orthographic views of the situation once we have transformed the bundle of rays and the world points to starting positions that will simplify the subsequent algebra.

## 5.2 Algebraic Form of the Revolving Motion

We will now think solely in terms of a transformation in the $xy$-plane that applies to the points while keeping the rays fixed. [2] The transformation we are after moves the world points from the configuration shown in Figure 6 to the configuration shown in Figure 7. The first two points are transformed onto their corresponding rays. The family of transformations that achieve this represents the revolving motion.

Let the slope of the projection of the second ray be $s$. The line equation of the projection is then

$$y = sx. \tag{1}$$

The transformation must maintain the first point on the $y$-axis. Let it position the first point at $y = m$. Moreover, let it position the projection line of the axis through the first two points such that the line equation of the projection is

$$y = kx + m, \tag{2}$$

[1] If the three image points and world points do not correspond to a true configuration, it is possible that the distance between the first two world points is smaller than the perpendicular distance between the first two rays. In this case, the above procedure is not possible and the pose problem has in fact no solution.

[2] That is, we consider a 3D transformation that affects all planes parallel to the $xy$-plane equally.

where $k$ is some slope. The transformation must also map the second point onto the second ray. Hence, the two lines (1) and (2) meet at the projection $(b, c)$ of the second point and this projection has $x$-coordinate $b$ such that

$$m = (s - k)b. \tag{3}$$

Let the projected distance between the first two world points be $D$. The situation is depicted in Figure 7. By inspecting

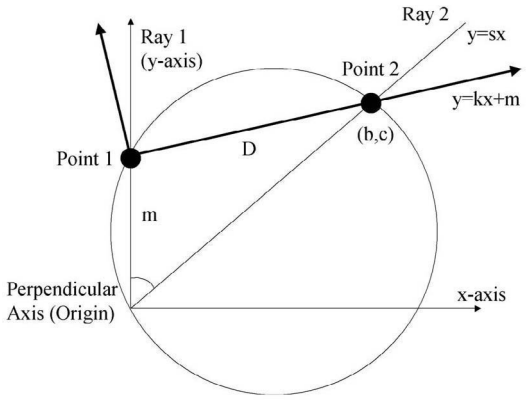


Figure 7: The situation after we have applied a valid transformation that brings the world points to one of the configurations arising from the revolving motion. The first world point is maintained on the first ray and the second world point now lies on the second ray.

the figure, it can now be seen that a valid transformation maps the $xy$-coordinates $(x, y)$ of a world point into the $xy$-coordinates $(\tilde{x}, \tilde{y})$ according to the formula

$$\begin{bmatrix} \tilde{x} \\ \tilde{y} \end{bmatrix} = \begin{bmatrix} 0 \\ m \end{bmatrix} + \frac{1}{D} \begin{bmatrix} b & -(c-m) \\ c-m & b \end{bmatrix} \begin{bmatrix} x \\ y \end{bmatrix}. \tag{4}$$

Let the scalar $u$ be defined by

$$u \equiv \frac{D}{b}. \tag{5}$$

Moreover, observe that by Pythagoras' Theorem we have $(k^2 + 1)b^2 = D^2$, which leads to

$$u^2 = 1 + k^2. \tag{6}$$

If we use Equations (2), (3) and (5), we can now rewrite the transformation in Equation (4) as

$$\begin{bmatrix} \tilde{x} \\ \tilde{y} \end{bmatrix} = \frac{1}{u} \left( \begin{bmatrix} 0 \\ (s-k)D \end{bmatrix} + \begin{bmatrix} 1 & -k \\ k & 1 \end{bmatrix} \begin{bmatrix} x \\ y \end{bmatrix} \right). \tag{7}$$

Thus, the one-dimensional family of valid transformations is parameterised by $u$ and $k$ under the constraint from (6).

### 5.3 The Effect on the Third Ray

The question is now which family of world points is mapped onto the third ray by the revolving motion. If we take Equation (7) and interpret the transformation as a full 3D-transformation that maps homogeneous coordinates $X = \begin{bmatrix} x & y & z & 1 \end{bmatrix}^\top$ of a world point into the new homogeneous coordinates $\tilde{X}$, we get

$$\tilde{X} = \begin{bmatrix} x - ky \\ k(x - D) + sD + y \\ uz \\ u \end{bmatrix}. \quad (8)$$

The transformed point $\tilde{X}$ lies on a plane $L = \begin{bmatrix} l_1 & l_2 & l_3 & l_4 \end{bmatrix}^\top$ if and only if $L^\top \tilde{X} = 0$, i.e.

$$a_1 + ka_2 + ua_3 = 0, \quad (9)$$

where

$$a_1 \equiv xl_1 + yl_2 + sDl_2 \quad (10)$$
$$a_2 \equiv xl_2 - yl_1 - Dl_2 \quad (11)$$
$$a_3 \equiv zl_3 + l_4. \quad (12)$$

The third image ray can be represented by two planes $L$ and $L'$ and if we define $a'_1, a'_2, a'_3$ analogously using $L'$ we have

$$a_1 + ka_2 + ua_3 = 0 \quad (13)$$
$$a'_1 + ka'_2 + ua'_3 = 0. \quad (14)$$

We eliminate $k$ and $u$, respectively, to obtain

$$u(a'_2a_3 - a_2a'_3) = (a_2a'_1 - a'_2a_1) \quad (15)$$
$$-k(a'_2a_3 - a_2a'_3) = (a_3a'_1 - a'_3a_1). \quad (16)$$

If we insert these two expressions into Equation (6), we get

$$(a_2a'_1 - a'_2a_1)^2 = (a'_2a_3 - a_2a'_3)^2 + (a_3a'_1 - a'_3a_1)^2, \quad (17)$$

which by the degree is readily seen to be the definition of a quartic surface. Since it is a union of lines, it is a ruled quartic surface. An example is shown in Figure 8.

We can now insert the equation for the plane of the circle to obtain a quartic curve in its plane. A circle has up to eight intersections with a quartic curve and these correspond to the solutions to the problem.

## 6. Algorithm Outline

An algorithm for finding the solutions to the generalised 3-point pose problem can now be discerned. The detailed numerical steps of the algorithm will be given in Section 7. Before we dive into the details, we summarise the main computational steps of the algorithm here:

1. Line up the rays in their canonical position.

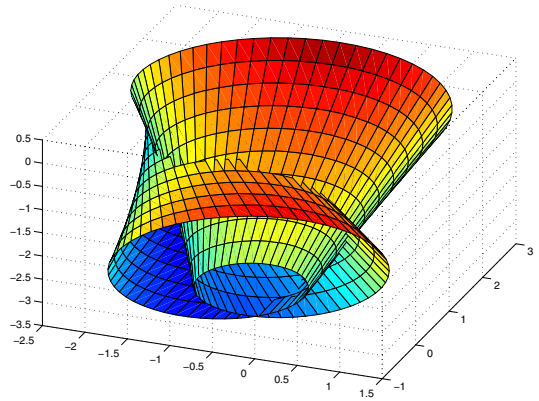

Figure 8: An example of the ruled quartic surface that is traced out by the third ray due to the revolving motion associated with the second degree of freedom. It is interesting to note that all sections parallel to the $xy$-plane are limaçons and that the vertices of the limaçons form a twisted cubic, part of which is a curve of self-intersection for the surface.

2. Line up the points in their canonical position.
3. Compute the coefficients of the two planes representing the third ray.
4. Compute the coefficients of an octic polynomial whose roots correspond to the intersections between the circle and the quartic surface.
5. Extract the roots of the octic polynomial.
6. Backsubstitute with each root to get the solutions for the transformation between the coordinate system of the points and the coordinate system of the rays.

## 7. Algorithm Details

We now give the detailed algebraic steps of the algorithm.

### 7.1. Lining Up the Rays

Let the rays be represented by the points $p_1$, $p_2$, $p_3$ on the rays and the unit direction vectors $d_1$, $d_2$, $d_3$. We wish to make $d_1$ parallel to the $y$-axis. The common perpendicular direction of the first two rays is

$$d_4 \equiv (d_1 \times d_2)/|d_1 \times d_2|, \quad (18)$$

which is the direction we wish to make parallel to the $z$-axis. Define also

$$d_5 \equiv d_1 \times d_4, \quad (19)$$

which is the direction that will then become parallel to the $x$-axis. The above will be accomplished if we rotate the rays by the rotation

$$R_1 \equiv \begin{bmatrix} d_5 & d_1 & d_4 \end{bmatrix}^\top. \quad (20)$$

The slope $s$ of the second ray as defined by (1) will be

$$s \equiv (d_1^\top d_2)/(d_5^\top d_2). \tag{21}$$

We also wish to place the point where the first ray meets the perpendicular axis at the origin. This point is given by

$$p_4 \equiv p_1 + \alpha d_1, \tag{22}$$

where

$$\alpha \equiv (d_1 - s d_5)^\top (p_2 - p_1). \tag{23}$$

The transformation that brings the rays to their starting position is hence

$$H_1 \equiv \begin{bmatrix} R_1 & -R_1 p_4 \\ 0 & 1 \end{bmatrix}. \tag{24}$$

We will henceforth assume that this transformation has already been applied to the rays.

## 7.2. Lining Up the Points

Let the world points be given as $q_1$, $q_2$, $q_3$. To bring them to their starting position, we first observe that the second ray now lies entirely in the $z$-plane whose $z$-coordinate $e$ is the third coordinate of $p_2$. Note also that

$$D \equiv \sqrt{|q_2 - q_1|^2 - e^2}. \tag{25}$$

Moreover,

$$d_6 \equiv \begin{bmatrix} D & 0 & e \end{bmatrix}^\top / |q_2 - q_1| \tag{26}$$

is a unit vector in the direction from the origin towards the point where we wish to position the second world point. Before the transformation, this direction is

$$d_7 \equiv (q_2 - q_1)/|q_2 - q_1|. \tag{27}$$

Define also

$$d_8 \equiv \begin{bmatrix} 0 & 1 & 0 \end{bmatrix}^\top \tag{28}$$

$$d_9 \equiv (d_7 \times (q_3 - q_1))/|d_7 \times (q_3 - q_1)|, \tag{29}$$

which are just unit vectors perpendicular to $d_6$ and $d_7$, respectively. Then our desired rotation is

$$R_2 \equiv \begin{bmatrix} d_6 & d_8 & (d_6 \times d_8) \end{bmatrix} \begin{bmatrix} d_7 & d_9 & (d_7 \times d_9) \end{bmatrix}^\top \tag{30}$$

and the transformation applied to the points is

$$H_2 \equiv \begin{bmatrix} R_2 & -R_2 q_1 \\ 0 & 1 \end{bmatrix}. \tag{31}$$

We will henceforth assume that this transformation has already been applied to the points.

## 7.3. Computing the Plane Coefficients

To compute the coefficients $L, L'$ for the two plane equations that represent the third ray, we find two distinct normal vectors $n, n'$ that are perpendicular to $d_3$. We pick $n$ as the vector of largest magnitude out of the two vector products $d_3 \times \begin{bmatrix} 1 & 0 & 0 \end{bmatrix}^\top$ and $d_3 \times \begin{bmatrix} 0 & 1 & 0 \end{bmatrix}^\top$. We then choose $n' \equiv d_3 \times n$ and the plane vectors are

$$L \equiv \begin{bmatrix} n^\top & -n^\top p_3 \end{bmatrix}^\top \tag{32}$$

$$L' \equiv \begin{bmatrix} n'^\top & -n'^\top p_3 \end{bmatrix}^\top. \tag{33}$$

## 7.4. Intersecting the Quartic and the Circle

We will now eliminate $x$ and $y$ from the quartic expression (17) in order to get an octic polynomial in $z$. [3] After lining up the points, the circle sits in the plane defined by

$$\begin{bmatrix} x & y & z \end{bmatrix} d_6 = q_3^\top d_6, \tag{34}$$

which gives

$$x = \kappa_1, \tag{35}$$

where

$$\kappa_1 \equiv -\frac{e}{D} z + \frac{|q_2 - q_1| q_3^\top d_6}{D}. \tag{36}$$

Moreover, the circle is the intersection between the plane and the sphere

$$x^2 + y^2 + z^2 = |q_3|^2. \tag{37}$$

If we insert Equation (35) into this, we get

$$y^2 = \kappa_2, \tag{38}$$

where

$$\kappa_2 \equiv |q_3|^2 - z^2 - \kappa_1^2. \tag{39}$$

By inserting Equation (35) into (10) and (11), we get

$$a_1 = y\kappa_3 + \kappa_4 \tag{40}$$

$$a_2 = y\kappa_5 + \kappa_6 \tag{41}$$

$$a_3 = \kappa_7 \tag{42}$$

$$a_1' = y\kappa_8 + \kappa_9 \tag{43}$$

$$a_2' = y\kappa_{10} + \kappa_{11} \tag{44}$$

$$a_3' = \kappa_{12}, \tag{45}$$

where

$$\kappa_3 \equiv l_2 \tag{46}$$

$$\kappa_4 \equiv l_1\kappa_1 + sDl_2 \tag{47}$$

$$\kappa_5 \equiv -l_1 \tag{48}$$

$$\kappa_6 \equiv l_2\kappa_1 - Dl_2 \tag{49}$$

$$\kappa_7 \equiv zl_3 + l_4 \tag{50}$$

$$\kappa_8 \equiv l_2' \tag{51}$$

$$\kappa_9 \equiv l_1'\kappa_1 + sDl_2' \tag{52}$$

$$\kappa_{10} \equiv -l_1' \tag{53}$$

$$\kappa_{11} \equiv l_2'\kappa_1 - Dl_2' \tag{54}$$

$$\kappa_{12} \equiv zl_3' + l_4'. \tag{55}$$

Using Equations (40)-(45) and (38) we then expand the expressions from Equation (17) as

$$a_2a_1' - a_2'a_1 = \kappa_{13}y + \kappa_{14} \tag{56}$$

$$a_2'a_3 - a_2a_3' = \kappa_{15}y + \kappa_{16} \tag{57}$$

$$a_3a_1' - a_3'a_1 = \kappa_{17}y + \kappa_{18}, \tag{58}$$

[3] We will work with polynomials in $z$ labeled $\kappa_i$. To implement the derivation of the octic, compute all the polynomials $\kappa_i$ in sequence.

where

$$\kappa_{13} \equiv \kappa_5\kappa_9 + \kappa_6\kappa_8 - \kappa_3\kappa_{11} - \kappa_4\kappa_{10} \quad (59)$$

$$\kappa_{14} \equiv \kappa_6\kappa_9 - \kappa_4\kappa_{11} + \kappa_2(\kappa_5\kappa_8 - \kappa_3\kappa_{10}) \quad (60)$$

$$\kappa_{15} \equiv \kappa_7\kappa_{10} - \kappa_5\kappa_{12} \quad (61)$$

$$\kappa_{16} \equiv \kappa_7\kappa_{11} - \kappa_6\kappa_{12} \quad (62)$$

$$\kappa_{17} \equiv \kappa_7\kappa_8 - \kappa_3\kappa_{12} \quad (63)$$

$$\kappa_{18} \equiv \kappa_7\kappa_9 - \kappa_4\kappa_{12}. \quad (64)$$

Squaring the right hand sides of Equations (56)-(58), inserting into Equation (17) and again using Equation (38) yields

$$\kappa_{19} = \kappa_{20} y, \quad (65)$$

where

$$\kappa_{19} \equiv \kappa_2(\kappa_{13}^2 - \kappa_{15}^2 - \kappa_{17}^2) + \kappa_{14}^2 - \kappa_{16}^2 - \kappa_{18}^2 \quad (66)$$

$$\kappa_{20} \equiv 2(\kappa_{15}\kappa_{16} + \kappa_{17}\kappa_{18} - \kappa_{13}\kappa_{14}). \quad (67)$$

By squaring Equation (65) and again using (38) we get

$$\kappa_{21} = 0, \quad (68)$$

where

$$\kappa_{21} \equiv \kappa_{19}^2 - \kappa_2\kappa_{20}^2, \quad (69)$$

which is an octic polynomial in $z$ whose roots correspond to the up to eight solutions.

### 7.5. Solving the Octic

A method for extracting the roots of a polynomial, which is easy to implement with most linear algebra packages, is to eigen-decompose a companion matrix. After normalising the polynomial so that it can be written

$$z^8 + \beta_7 z^7 + \beta_6 z^6 + \ldots + \beta_0, \quad (70)$$

the roots are found as the eigenvalues of the $8\times8$ companion matrix

$$\begin{bmatrix} -\beta_7 & -\beta_6 & \cdots & -\beta_0 \\ 1 & & & \\ & \ddots & & \\ & & 1 & \end{bmatrix}. \quad (71)$$

More efficient however, is to find the roots using Sturm sequences. For more details, the reader is referred to [12], where this was done for a tenth degree polynomial.

### 7.6. Backsubstitution

For each solution for $z$ we can compute $x$ by Equation (35) and $y$ by Equation (65). Then $u$ and $k$ can be computed using Equations (15) and (16), respectively. The transformation defined in Equation (7) is then uniquely determined. We label it $H_3$. For each solution, we also need to find the transformation $H_4$ that rotates the third world point $q_3$ around to the correct point on the circle. Define

$$d_{10} \equiv (d_6 \times \begin{bmatrix} x & y & z \end{bmatrix}^\top)/|d_6 \times \begin{bmatrix} x & y & z \end{bmatrix}^\top|. \quad (72)$$

Then our desired rotation is

$$R_4 \equiv \begin{bmatrix} d_6 & d_{10} & (d_6 \times d_{10}) \end{bmatrix} \begin{bmatrix} d_6 & d_8 & (d_6 \times d_8) \end{bmatrix}^\top \quad (73)$$

and the transformation applied to the points is

$$H_4 \equiv \begin{bmatrix} R_4 & 0 \\ 0 & 1 \end{bmatrix}. \quad (74)$$

The full transformation from the coordinate system of the points to the coordinate system of the rays is finally

$$H = H_1^{-1} H_3 H_4 H_2. \quad (75)$$

## 8. Relation to the Classical Case

In the classical case, the circle has its centre in the $xy$-plane and the plane of the circle is perpendicular to the $xy$-plane. The quartic surface also has a symmetry property in the classical case. An example is shown in Figure 9. The revolving motion rotates the direction of the third ray by only 180 degrees while revolving the projection centre around the complete circle, i.e. it takes two full laps for the third ray to return to its initial position. After one lap, the third ray can be thought of as reflected across the $xy$-plane. Hence, in the classical case, both the circle and the quartic surface are unaffected by a reflection across the $xy$-plane. In other words, for any intersection point $(x, y, z)$ there is a corresponding intersection $(x, y, -z)$. The corresponding intersection represents the reflection of the camera projection centre across the plane defined by the three world points. Due to the symmetry, all the odd order terms of the octic polynomial in Equation (68) have to vanish. This means that the octic can be considered a quartic in $z^2$ and the roots can hence be found in closed form. Moreover, it is seen that our generalised solution can handle the classical case seamlessly, without identifying it explicitly.

## 9. The Orientation Constraints

In practical situations, there are typically orientation constraints arising from the requirement that the world points should be in the forward direction from the camera. Let a camera ray be represented by the point $p$, which is where the ray enters the camera, and the forward direction $d$. The world point $q$ is then on the correct part of the ray when

$$d^\top(q - p) > 0. \quad (76)$$

Once the tentative solutions have been extracted, it is straightforward to test which ones satisfy the orientation constraints. In the classical case, this singles out at most one solution from each pair [4], leaving up to four solutions.

[4] Using the projection centre as $p$ for all rays.

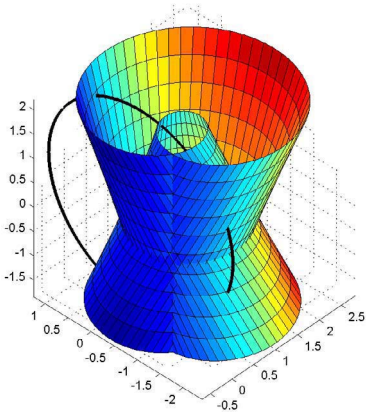

Figure 9: In the classical case, both the circle and the quartic are symmetric with respect to reflection in the $xy$-plane. The solutions therefore come pairwise as reflections of each other across the $xy$-plane. As a result, all the odd order terms of the octic polynomial vanish and the solutions can be found in closed form. The self-intersection curve degenerates to a circle and a line.

# 10. Experimental Verification

The main requirements on a minimal method such as this one are numerical accuracy and speed. Note that all minimal solutions will behave similarly with respect to noise. The numerical precision is investigated in Figure 10.

The majority of the computation effort is spent on finding the roots of the octic polynomial. An efficient implementation using Sturm sequences can find the roots in less than $25\mu s$ on a machine with a $3GHz$ processor. The computation time is partially dependent on the number of real solutions. The distribution of the number of valid solutions with random configurations is investigated in Figure 11.

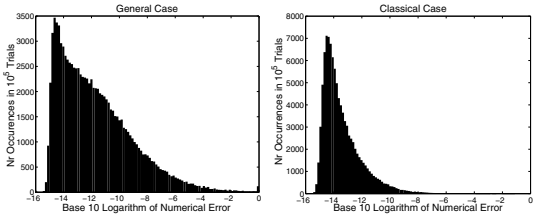


Figure 10: The distribution of numerical error (in terms of Frobenius norm) in the computed $H$ based on $10^5$ trials with random general and classical configurations of unit scale. In the general case, the error is below $10^{-6}$ for 96.3% of the trials. In the classical case, which was not explicitly detected, the error is below $10^{-6}$ for 99.9% of the trials.

# 11. Conclusion

We have presented a generalised solution to the 3 point pose problem, which works for any type of camera geometry, such as for example a camera facing an arbitrarily shaped mirror. The generalisation removes all restrictions on the three rays into the camera, whereas in the classical case, they have to be concurrent in a projection centre. The general solution can handle the classical case seamlessly, without explicitly identifying it and without any numerical problems. The intended use for the algorithm is in a hypothesise-and-test architecture to solve robustly for camera pose.

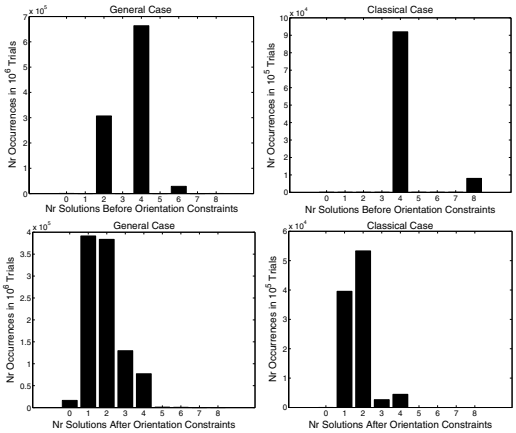


Figure 11: Distribution of number of valid solutions with random general and classical configurations, before and after the orientation constraints have been enforced. In the bottom row, a misalignment of $10^{-6}$ or less was required between all rays and their corresponding points, which is the reason for the cases without solutions. In the general case, the number of trials with eight solutions is tiny but non-zero even with the orientation constraints.

# References


[1] E. Adelson and J. Bergen, The Plenoptic Function and the Elements of Early Vision, In *Computational Models of Visual Processing*, ISBN 0-262-12155-7, MIT Press, 1991.

[2] T. Alter, 3-D Pose from 3 Points Using Weak Perspective, *IEEE Transactions on Pattern Analysis and Machine Intelligence*, Vol. 16, No.8, pp. 802-808, 1994.

[3] P. Baker, R. Pless, C. Fermüller and Y. Aloimonos, Eyes from Eyes, *SMILE 2000, LNCS 2018*, pp. 204-217, 2001.

[4] Euclid, *The Elements*.

[5] O. Faugeras, *Three-Dimensional Computer Vision: a Geometric Viewpoint*, MIT Press, ISBN 0-262-06158-9, 1993.

[6] M. Fischler and R. Bolles, Random Sample Consensus: a Paradigm for Model Fitting with Application to Image Analysis and Automated Cartography, *Commun. Assoc. Comp. Mach.*, 24:381-395, 1981.

[7] M. Grossberg and S. Nayar, A General Imaging Model and a Method for Finding its Parameters, *IEEE International Conference on Computer Vision*, Volume 2, pp. 108-115, 2001.

[8] A. Gruen and T. S. Huang, *Calibration and Orientation of Cameras in Computer Vision*, Springer Verlag, ISBN 3-540-65283-3, 2001.

[9] J. Grunert, Das Pothenotische Problem in erweiterter Gestalt nebst über seine Anwendungen in der Geodäsie, *Grunerts Archiv für Mathematik und Physik* 1, 238-248, 1841.

[10] R. Haralick, C. Lee, K. Ottenberg and M. Nölle, Review and Analysis of Solutions of the Three Point Perspective Pose Estimation Problem, *International Journal of Computer Vision*, 13(3):331-356, 1994.

[11] R. Hartley and A. Zisserman, *Multiple View Geometry in Computer Vision*, Cambridge University Press, ISBN 0-521-62304-9, 2000.

[12] D. Nistér. An Efficient Solution to the Five-Point Relative Pose Problem, *IEEE Conference on Computer Vision and Pattern Recognition*, Volume 2, pp. 195-202, 2003.

[13] D. Nistér. Preemptive RANSAC for Live Structure and Motion Estimation, *IEEE International Conference on Computer Vision*, pp. 199-206, 2003.

[14] R. Pless, Using Many Cameras as One, *IEEE Conference on Computer Vision and Pattern Recognition*, Volume 2, pp. 587-593.



The views and conclusions contained in this document are those of the authors and should not be interpreted as representing the official policies, either expressed or implied, of the Army Research Laboratory or the U. S. Government.